Smart Materials and Structures



**PAPER** • **OPEN ACCESS**

# Analyzing the influence of the core pre-structure on the dynamic response of a magnetorheological elastomer sandwich structure

To cite this article: Narongdet Sulatchaneenopdon *et al* 2022 *Smart Mater. Struct.* **31** 075027



OPEN ACCESS
IOP Publishing
Smart Materials and Structures
Smart Mater. Struct. **31** (2022) 075027 (16pp)
https://doi.org/10.1088/1361-665X/ac775b

# Analyzing the influence of the core pre-structure on the dynamic response of a magnetorheological elastomer sandwich structure

**Narongdet Sulatchaneenopdon[1,*], Zhiming Shen[1], Hyoung-Won Son[1], Anak Khantachawana[2], Jon Garcia-Barruetabena[3], Maria Jesus Elejabarrieta[3], Tsutomu Takahashi[4], Tadachika Nakayama[1,*] and Koichi Niihara[1]**

[1] Extreme Energy-Density Research Institute, Nagaoka University of Technology, Nagaoka, Niigata 940-2188, Japan
[2] Department of Mechanical Engineering, King Mongkut's University of Technology Thonburi, 10140 Bangkok, Thailand
[3] Department of Mechanics, Design and Industrial Management, University of Deusto, Avda. de las Universidades 24, 48007 Bilbao, Spain
[4] Department of Mechanical Engineering, Nagaoka University of Technology, Nagaoka, Niigata 940-2188, Japan

E-mail: s197011@stn.nagaokaut.ac.jp and nky15@vos.nagaokaut.ac.jp

Received 19 March 2022, revised 16 May 2022
Accepted for publication 9 June 2022
Published 21 June 2022

**Abstract**

Recently, vibration control has been useful in various engineering fields such as aerospace, adaptive dynamic vibration absorbers, and infrastructure. Magnetorheological elastomer (MRE) is an interesting material for controlling and suppressing undesirable vibrations through the application of a magnetic field. The present study aims at analyzing the pre-structure of the magnetorheological viscoelastic core in the dynamic response of an MRE-sandwich structure. The forced vibration tests were performed under a non-homogenous magnetic field to evaluate the dynamic properties of the MRE-sandwich structure in a frequency bandwidth range of 0–250 Hz. Experimental results show that the proposed MRE-sandwich structures are capable of eliminating unwanted resonances due to induced magnetic field intensity in the activated region, especially at the fundamental mode. Moreover, results highlight that an oriented pre-structure in an MRE-sandwich has an attenuation effect on vibrations in the low frequency range. Additionally, the external magnetic field increased the structural vibrations damping capability by approximately 200%. In addition, the oriented pre-structures of the MRE core were also used to dissipate vibration. Consequently, they could potentially be used in vibration attenuation applications such as stop operations in dynamic structures.

* Authors to whom any correspondence should be addressed.



 

Supplementary material for this article is available online

Keywords: magnetorheological elastomer, sandwich structure, oriented pre-structure, vibration attenuation

(Some figures may appear in colour only in the online journal)

## 1. Introduction

Vibration control is an alternative method to eliminate unwanted resonances or avoid structural failures originating from mechanical vibrations. Passive damping treatment with viscoelastic materials has been successfully applied in structural vibration control because of its cost-effectiveness and requirement of fewer manufacturing steps.

Usually, a conventional viscoelastic layer is constrained between two rigid layers to form a sandwich that can dissipate energy by structural deformation in shear mode. The viscoelastic sandwich structure is generally designed to accomplish a suitable performance, diminish noise radiation, have good reliability, and extend service life. These sandwich structures are crucial in a number of industrial applications, such as infrastructure, automotive, and aeronautical applications, because they offer superior damping-to-weight, strength-to-weight, and stiffness-to-weight ratios [1].

With the technological development of materials and processes, a new class, so-called smart materials, has been introduced. These materials can respond in a reversible and controllable manner, modifying some of their properties under the influence of external stimuli [2]. Due to their unique and useful actuator properties, smart materials such as piezoelectric (response to electricity and pressure), shape memory alloys (response to thermal and pressure), electrostrictive materials (response to electric field), magnetostrictive materials (response to magnetic field), electrorheological (ER) materials (react to electric field), and magnetorheological (MR) materials (react to magnetic field) have gained considerable attention in a broad range of engineering applications.

Magnetorheological elastomers (MREs) are smart materials that consist of ferromagnetic particles added to a non-magnetic matrix. Rheological properties of an MRE material can be changed continuously, rapidly, and reversibly by means of an external magnetic field. MREs are classified as isotropic or anisotropic according to the spatial distribution of the magnetic particles during the curing process. A homogenous distribution without a magnetic field allows an isotropic structure, whereas a chain-like columnar structure in the presence of a magnetic field provides an anisotropic structure [3–13]. Stiffness and damping properties of MREs can be controlled by adjusting the strength of the magnetic field [3, 5, 10–12]. Moreover, these materials have many advantages such as quick response within milliseconds and superior dynamic response variation, which are potentially appropriate for adaptive tuned vibration structures and devices [8]. MREs exhibit the superior characteristic of being able to simultaneously change the damping and stiffness of the structure, which makes them candidates for vibration control materials [1, 2, 7]. Recent studies have focused on the enhancement of magnetorheological properties. The effect of particle chain network formation in a non-magnetizable matrix has been extensively studied. The anisotropic structure was found to exhibit a higher storage modulus relative MR effect as compared to the identical isotropic structure but a higher loss modulus for the same matrix with the same percentage amount of particles [14, 15]. Anisotropic structures with large particles exhibited higher damping properties than smaller particles [16–18]. Boczkowska *et al* [17] and Tian and Nakano [19] reported the improvement in the rheological properties of MREs by varying the alignment of carbonyl iron particles (CIPs) (0°, 30°, 45°, 90°, and isotropic). Zhang *et al* [20] reported the magneto-mechanical properties of MREs containing minor oriented alignment CIPs (0°, 5°, 10°, and 15°). Results showed that the mechanical properties of MREs strongly depended on the particle orientation structures.

Design parameters of viscoelastic sandwich structures on dynamic behaviors, such as performance and damping capability, have been studied in the recent decades. Kerwin [21] and Ungar [22] predicted the damping effectiveness of the viscoelastic sandwich using an analytical model. Many researchers consequently investigated the influence of frequency, environmental temperature, and properties of sandwich structures such as the thickness of the viscoelastic layer [23], types of metallic skin [24, 25] in the region of linear vibration [26, 27], and non-linear vibration [28–30]. Current research has concentrated on the optimal design for multi-layered sandwich structures to attain certain goals, such as minimizing mass while maximizing damping [31–34]. However, the optimal design cannot reach the required damping because it is based on structural mass, damping, and mechanical properties.

To overcome this limitation, active and MRE damping treatment and vibration control strategies have been proposed in sandwich structures embedded with novel types of intelligent viscoelastic layers [35]. Conventional cores are being replaced by smart sandwich structures, which can modify their dynamic properties in response to external stimuli, using magnetorheological material [36, 37], ER materials [38–40], or shape memory alloy [41]. Yeh [42] studied a vibration analysis of a rectangular sandwich plate with MRE viscoelastic film. MRE has a significant effect on vibration characteristics of the sandwich beam. A more significant vibration reduction can be achieved in a cantilever beam and only the first mode frequency decreases when the non-homogeneous magnetic field moves a position from the fixed end towards the free end [43–46]. Chikh *et al* [47] discovered that the damping coefficient and shear modulus increased by application of a magnetic field. Aguib *et al* [48] studied the influence of MRE

adaptive stiffness and loss factor of a sandwich structure on the parametric instability region for the first three modes of vibration. Gurgen and Sofuoglu [49] studied vibration attenuation properties of a smart fluid-based sandwich structure due to shear thickening mechanism at low temperature. Rokn-Abadi *et al* [50] validated the effect of magnetic field intensity, thickness of the core and magnetoelastic loads on the dynamic behavior of MR-based sandwich beam by using Hamilton's principle. Li *et al* [51] predicted and evaluated through analytical modeling of free and forced vibration properties of MRE-composite structural system by simultaneously accounting for internal magnetic field and temperature. Zhang *et al* [52] investigated the dynamic performance of aluminum shallow shell panel, which have been shown experimentally to be significantly influenced by the effect of magnetic field, initial curvature, and forcing amplitude. Subramani *et al* [53] studied the dynamic behavior of a spherical MRE sandwich shell panel, in which MRE is demonstrated to be effective in controlling vibration and damping. Selvaraj *et al* [54] investigated the vibration and damping characteristics of the rotating laminated composited hybrid MR elastomer sandwich panel. Wang *et al* [55] successfully developed a novel sandwich beam by using a periodically arranged MRE-coil oscillator for vibration suppression, which investigated the local resonance band gap in real-time. Several studies have also improved dynamic properties and damping performance by using MRE reinforced with particle carbon nanotubes or graphene nanoplatelets [53, 54, 56, 57]. In addition, several studies have concentrated on the vibration attenuation in structures using the magnetic field-dependent shear modulus of the viscoelastic layer resulting in a change in the stiffness and damping characteristics [43, 44, 47, 48, 58–60].

The novelty of the present research consists in studying the influence of the MRE-viscoelastic core pre-structure on the magnetic field interactions generated by the dynamic response of the MRE-sandwich. The influence of design parameters was experimentally characterized in a low-frequency bandwidth range of 0–250 Hz. A localized magnetic field was generated by inducing several intensities to prove their efficiency in attenuating structural vibration. In addition, in the present study we observed structural motion using a high-speed microscope. The vibrational behavior of MRE-sandwich structures is established based on the dynamic properties following the ASTM E756-05 standard test method [61]. Moreover, the effect of oriented pre-structures embedded in MRE structure was also discussed.

## 2. Manufacturing and characterization

The magnetorheological structures used in the present study were manufactured to investigate the dynamic properties of the MRE-sandwich structure and MRE cores by forced vibration measurement with resonance according to ASTM E756-05. One isotropic and four anisotropic MRE cores were synthesized and embedded in symmetrical aluminum skins. This section will describe the manufacturing and experimental techniques designed to identify the material properties of the MRE-sandwich structure.

### 2.1. Fabrication of the magnetorheological elastomer (MRE) material

In the present study, the starting materials YE5822A (silicone base) and YE5822B (curing agent) were obtained from Momentive Co., Ltd The silicone and curing agent were mixed at a ratio of 10:1. The viscosity and apparent density of the matrix were 1.2 Pa s at 23 °C and 0.97 g $cm^{-3}$, respectively. The dispersed particles are spherical CIPs (FEE16PB, Purity: 99.9%), which have a diameter of 3–5 $\mu$m (Kojundo Chemical Laboratory Co., Ltd, Japan). The apparent density and saturation magnetization of the CIPs were 7.87 g $cm^{-3}$ and 146 emu $g^{-1}$, respectively. To uncured silicone (YE5822A), 10 vol% of carbonyl iron powder was mixed for 30 min using a hybrid mixer. A well-homogenous mixture was degassed in a vacuum incubator for 30 min to eliminate microbubbles. The curing agent (YE5822B) was added to a mixture by sonication bath for 5 min, which is the synthesis method of MRE-sandwich core as represented in figure 1 (step 1 through step 4). Finally, the mixture was cast into a 0.5 mm × 20 mm × 20 mm mold under an external magnetic field (450 mT) for 4 h at 70 °C [62]. Analysis of x-ray CT scanning images is an alternative method to evaluate the pre-structure orientation of CIPs-containing MRE-sandwich core, as illustrated in figure 2. Visible white domains correspond to the localized CIPs position in the MRE-sandwich core, which form a network under magnetic field application (450 mT). The pre-structure control of anisotropic and isotropic structures of MRE-sandwich core were confirmed in figure 2(A) through 2(E).

### 2.2. Fabrication of the MRE-sandwich structure

The MRE-sandwich structure was made of symmetrical aluminum skin and a magnetorheological core. The mixture was prepared by fabrication of MRE material sections before the curing process, as shown in figure 1 (step 5 and step 6). The mixture was coated onto aluminum plates like viscoelastic film in a prepared mold. Pre-structure control of anisotropic MRE-sandwich structures was accomplished using a magnetic field (450 mT), whereas isotropic MRE-sandwich structures were cured in the absence of any magnetic field. In figures 3(A)–(D), the magnetorheological core is aligned in the direction of the magnetic field $\theta$. The value of $\theta$ was defined for several anisotropic specimens as 0°, 30°, 45°, and 90°. After the curing process of the material, specimens were carefully removed from the mold to avoid delamination. The dimensions of the MRE-structure are illustrated in figure 4, where *b, L*, and *H* are the width, length, and thickness of the MRE-sandwich, and $H_v$ and $H_e$ are the thicknesses of the MRE film and the metallic skin, respectively. Table 1 shows the physical properties of MRE-sandwich structures, and the components of these structures are specified. $E_e$ is the storage modulus of metallic skin, and $\rho$, $\rho_v$, and $\rho_e$ are the densities of the sandwich structure, the

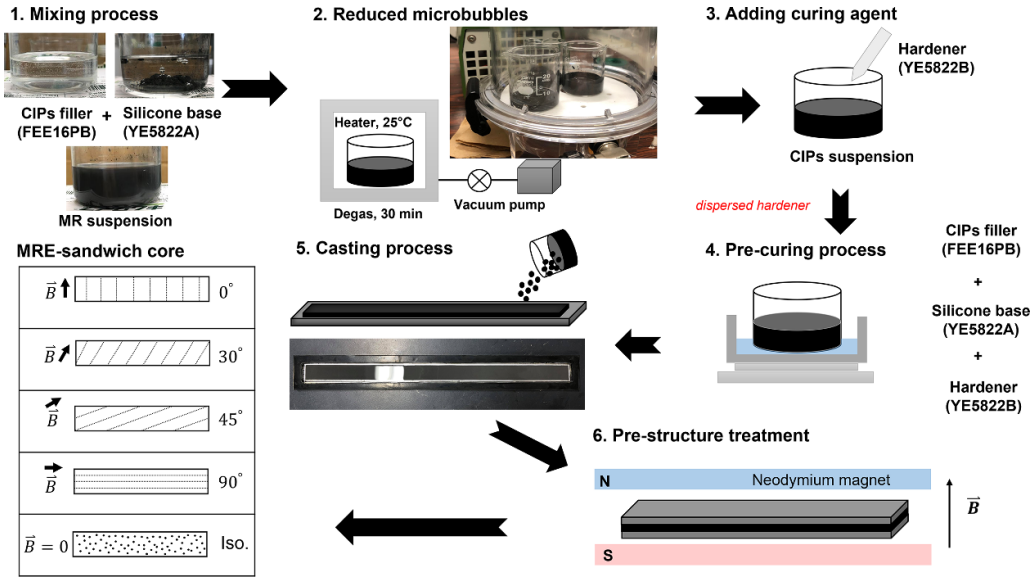


**Figure 1.** Pre-structure control of sandwich structure by non-homogeneous magnetic field treatment.

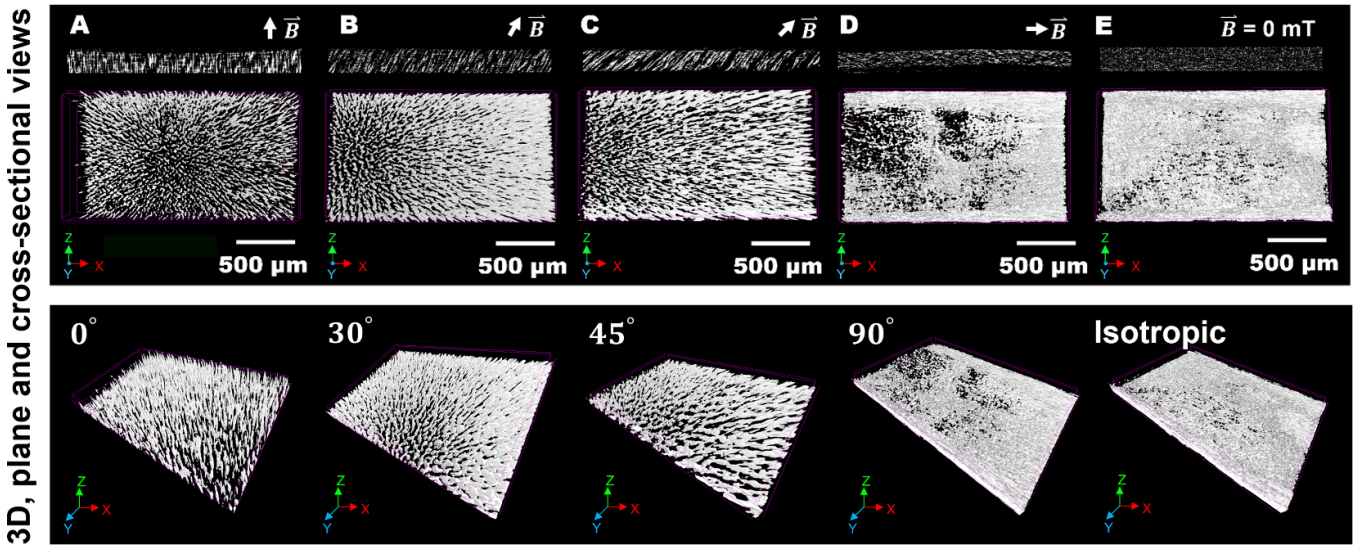


**Figure 2.** The x-ray CT micrograph of magnetorheological (MRE) sandwich core (A) 0°, (B) 30°, (C) 45°, (D) 90° and (E) isotropic.

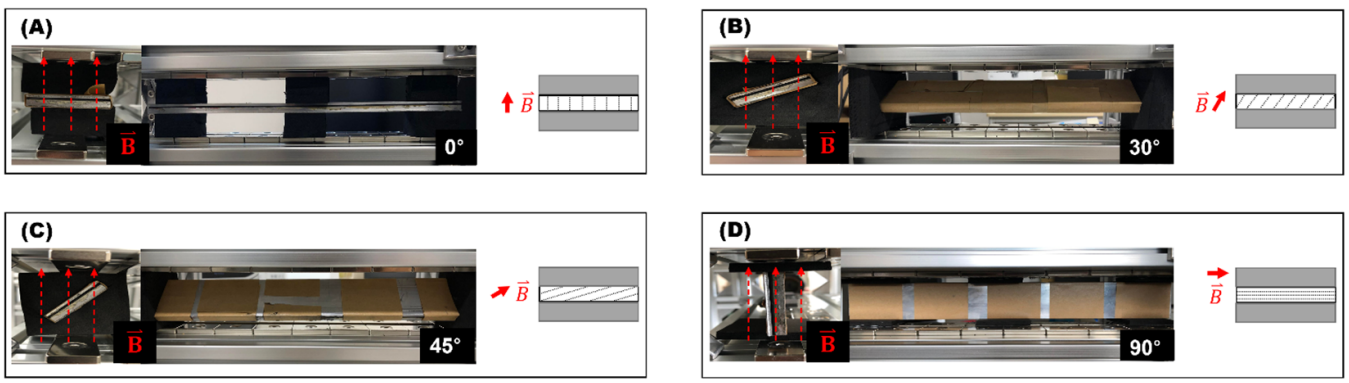


**Figure 3.** Pre-structure control of anisotropic structure of MRE-sandwich core (A) 0°, (B) 30°, (C) 45° and (D) 90°.

**Table 1.** Specifications of composite beams.

| | Sandwich | | | Aluminum skin | | | MRE layer | |
|---|---|---|---|---|---|---|---|---|
| Sample | $H$ ($\pm$0.03 mm) | $b$ ($\pm$0.1 mm) | $\rho$ (g cm$^3$) | $H_e$ ($\pm$0.03 mm) | $\rho_e$ (g cm$^3$) | $E_e$ (GPa) | $H_v$ ($\pm$0.03 mm) | $\rho_v$ ($\pm$0.01 g cm$^3$) |
| 0° | 1.39 | 20 | 2.43 | 0.51 | 2.7 | 71 | 0.38 | 1.8 |
| 30° | 1.37 | 20 | 2.34 | 0.51 | 2.7 | 71 | 0.36 | 1.6 |
| 45° | 1.40 | 20 | 2.37 | 0.51 | 2.7 | 71 | 0.39 | 1.8 |
| 90° | 1.41 | 20 | 2.38 | 0.51 | 2.7 | 71 | 0.40 | 1.9 |
| Isotropic | 1.38 | 20 | 2.27 | 0.51 | 2.7 | 71 | 0.37 | 1.7 |


**Figure 4.** Configuration of the magnetorheological elastomer (MRE)-sandwich structure.

metallic skin, and the MRE core, respectively. The composite beam specifications are summarized in table 1.

### 2.3. Experimental setup

MRE-sandwich specimens in a free-free beam configuration were characterized according to the ASTM E756-05 standard as the preferred method for determining the frequency response function. A seismic base motion was used to substitute the excitation force for the clamp in the present study, as well as to prove that the procedure works equally well with transmissibility functions [63]. Note that all of the characterizations have been carried out in the linear viscoelastic range. In the experimental study, the modal behavior of MRE-sandwich specimens with five oriented pre-structures of the MRE layer was determined by forced vibration. Figures 5(A) and (B) show a diagram of the designed experimental setup, which includes a mini smart shaker (Model: K2004E1), an electromagnet, a power supply, a 30 MHz multifunction generator, a high-speed microscope (Model: VW-600C), and a motion signal analysis monitor (Model: VW-9000NN). A distance of 200 mm from the free end of the MRE-sandwich beam was clamped by the mini smart shaker, and the free end was excited between electromagnet poles. The excited motion was stimulated by using the mini smart shaker with an entire frequency bandwidth from 0 to 250 Hz. A sinusoidal signal was generated for driving the shaker by the 30 MHz multifunction generator as a function of frequency with an increased resolution of 0.1 Hz s$^{-1}$. An excited motion at a specific point in real time was observed with the high-speed microscope. Data acquisition and signal processing as a velocity-time function were evaluated with a motion signal analysis monitor. The resolution control of excitation amplitude is lower in the fundamental frequency mode (first vibration mode) compared to high-frequency modes (second and third vibration modes). The excitation signal was set at 200 mV in fundamental frequency mode and increased up to 1000 mV at high-resonant-frequency modes. The high-speed microscope is capable of collecting vibrational displacements easier and more precisely in higher-frequency modes rather than in the first frequency mode.

The characterization of MRE-sandwich structures were assessed in a non-uniform magnetic field introduced in the local area at the free end by a current feed to the electromagnet field from 0 A (0 mT) to 0.8 A (240 mT). OriginPro programming was used for the analysis of all obtained vibration signals. Several transient response parameters were evaluated, including frequency and time domains. Moreover, the dynamic properties of all sandwich structures were obtained according to the ASTM E756-05 standard. The storage modulus is given by

$$E = \frac{12\rho L^4 {f_n}^2}{H^2 {C_n}^2}, \tag{1}$$

where $\rho$ is the density of the MRE-sandwich, $H$ is the total thickness of the MRE-sandwich, $L$ is the free length, $f_n$ is the resonance frequency of mode $n$, and $C_n$ is the coefficient for mode n of clamped-free configuration. The loss factor $\eta$, which is also frequency dependent, is obtained by the half-power bandwidth method. In this method, the modal loss factor, $\eta$, is obtained by the division of the bandwidth, where the amplitude of the peak was reduced by 3 dB, $\Delta f_n$, at the resonance frequency. The loss factor ratio of the frequency to the resonance frequency is given by

$$\eta = \frac{\Delta f_n}{f_n}. \tag{2}$$

Finally, assuming that the MRE-sandwich shows linear viscoelastic behavior, the combined complex modulus is expressed as

$$E^*(f_n) = E(f_n) \bullet (1 + i\eta(f_n)). \tag{3}$$

This experiment was performed with three specimens for each oriented pre-structure to improve the accuracy of the results. The present study presented a novel technique to observe

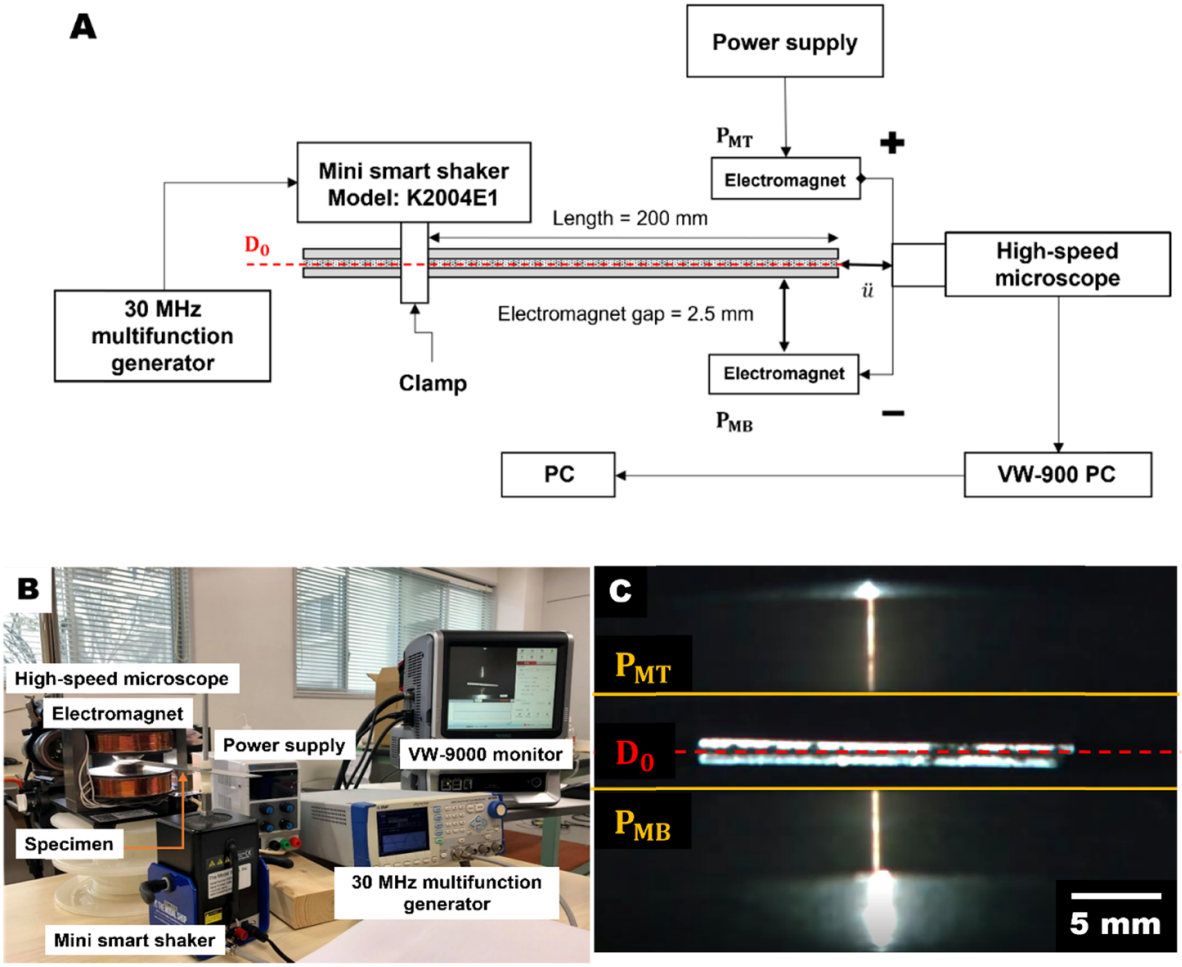


**Figure 5.** Experimental setup for the MRE-sandwich beam. (A) Forced vibration diagram, (B) vibration testing station, and (C) vibrational motion of MRE-sandwich with a high-speed microscope under an electromagnetic pole.

structural motion using a high-speed microscope because this equipment displays the slow-motion mode in real time and does not influence the total mass of the system. Moreover, the proposed technique does not affect the vibration result, so the apparatus is better than a laser vibrometer or accelerometer. Figure 5(C) demonstrates the vibrational motion of the MRE-sandwich under an electromagnetic pole using a high-speed microscope, where $D_0$ is the origin position of the specimen, $P_{MT}$ and $P_{MB}$ are the top and bottom positions of electromagnetic probe, respectively.

## 3. Results and discussion

### 3.1. Magnetorheological properties

The MRE material was deformed by shear stress and shear strain in the pre-yield regime. The stress–strain relationship based on linear viscoelastic theory is given by

$$\tau = G^* \gamma, \tag{4}$$

where $\tau$ is the shear stress, $\gamma$ is the shear strain, and $G^*$ is the complex modulus represented by

$$G^* = G' + iG'', \tag{5}$$

where $G'$ is the storage modulus, and $G''$ is the loss modulus.

The loss factor ($\tan\delta$) is the relationship between the loss and storage moduli, which is given as follows

$$\tan\delta = \frac{G'}{G''}. \tag{6}$$

Results were obtained using an MCR302 rheometer from Anton Paar GmbH equipped with an MR cell (MRD-1T). The apparatus used was a parallel disc configuration (20 mm diameter) and a gap of 0.40 mm, which is the thickness of MRE samples. The MRE sample characterization was performed using 50 points from 0.01% to 10% spaced logarithmically, and each point was measured for 5 s. During all subsequent measurements, the temperature was maintained constant at 25 $\pm$ 0.5 °C. An external magnetic field was applied to a sample along the axial direction by increasing the magnetic field intensity from 0 mT to a maximum of 240 mT.

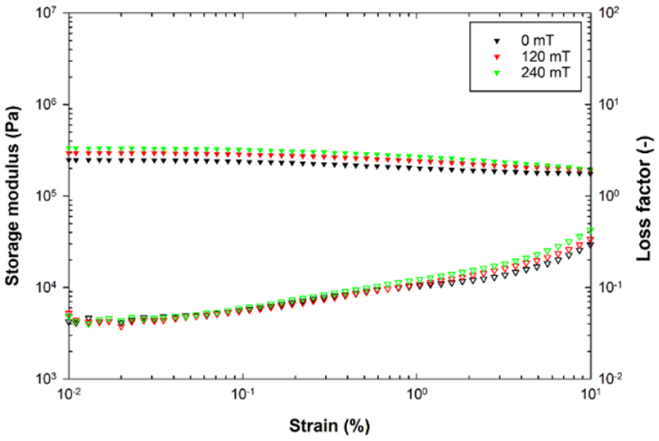


**Figure 6.** Viscoelastic properties on the storage modulus (▼) and loss factor (▽) of the representative pre-structure (30°) as a function of strain amplitude.

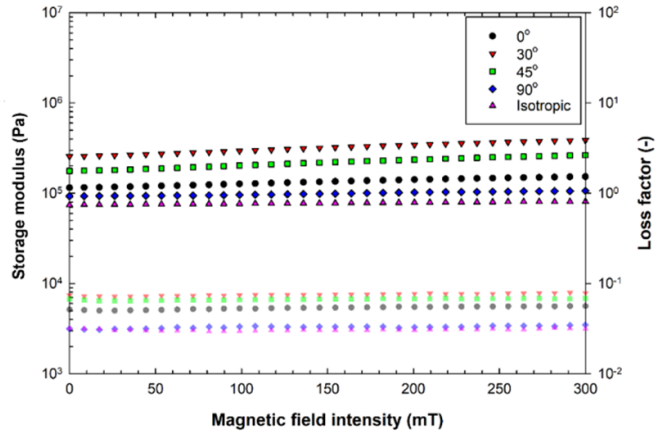


**Figure 7.** Viscoelastic properties of the MRE, 0° (●), 30° (▼), 45° (■), 90° (♦), and isotropic (▲) at constant shear strain (0.01%) and excitation (5 Hz) under pre-structures having various orientations as a function of the magnetic field.

Figure 6 shows the relationship between viscoelastic properties (storage modulus and loss factor) and strain under different magnetic fields. The result shows an increment of the magnetic field-induced viscoelastic properties. The main reason is that the magnetic force reduced the distance between adjacent particles, and the MRE induced local deformation [11, 36]. Furthermore, the MRE has a slightly higher sensitivity to the magnetic field and the alignment of ferromagnetic particles [64].

In figure 7, the storage moduli and loss factor are plotted against the magnetic field when the shear strain and excitation frequency remained constant at 0.01% and 5 Hz, respectively. The result shows that the storage and loss moduli increased slightly with the increment of magnetic field intensity. Moreover, a larger initial angle $\theta$ of the oriented pre-structure induces a larger shear modulus because the alignment angle of the particle chains offers restriction mobility of the matrix by incrementing the alignment angle $\theta$ [17, 62].

### *3.2. Dynamic analysis of the MRE-damping sandwich*

In this section, the modified resonant frequency is analyzed by fast Fourier transform (FFT) spectrum of the time response signal. The modified resonance frequency of the MRE-sandwich for variously oriented pre-structures and magnetic field intensity are listed in table 2. With increasing magnetic fields, the first resonance frequency of all oriented pre-structure in MRE-sandwich core will be decremented more dramatically due to a magneto-elastic force on the CIPs contained in the elastomer [43, 65]. It is noted that the micro-mechanism of the MRE-sandwich core exhibited shear motion due to the particle movement in the matrix during an application of a magnetic field [11]. MRE-core stiffness changes when magnetic field intensity is induced in MRE-sandwich structure, thus reducing the resonance frequency. This phenomenon affected the structural composite beam in the fundamental mode (first vibration mode). However, the second and

**Table 2.** Resonance frequencies of magnetorheological elastomer (MRE)-sandwich structures.

| | | Magnetic field intensity (mT) | | | | | |
|---|---|---|---|---|---|---|---|
| | | 0 | | 120 | | 240 | |
| Sample | Mode No. | $f_n$ | $\Delta\omega$ (%) | $f_n$ | $\Delta\omega$ (%) | $f_n$ | $\Delta\omega$ (%) |
| 0° | 1 | 21.11 ± 0.39 | — | 20.50 ± 0.61 | 3.02 ± 4.95 | 18.26 ± 1.94 | 16.39 ± 14.53 |
| | 2 | 94.94 ± 3.22 | — | 94.94 ± 3.35 | 0.13 ± 0.14 | 94.88 ± 3.27 | 0.06 ± 0.05 |
| | 3 | 206.61 ± 2.82 | — | 206.83 ± 3.05 | 0.18 ± 0.11 | 206.79 ± 3.66 | 0.37 ± 0.40 |
| 30° | 1 | 21.59 ± 0.35 | — | 20.79 ± 0.24 | 3.85 ± 0.50 | 18.76 ± 0.76 | 15.17 ± 2.76 |
| | 2 | 96.25 ± 2.20 | — | 96.20 ± 2.36 | 0.05 ± 0.16 | 96.28 ± 2.14 | 0.04 ± 0.07 |
| | 3 | 207.51 ± 1.41 | — | 207.40 ± 1.36 | 0.05 ± 0.03 | 207.55 ± 1.29 | 0.02 ± 0.06 |
| 45° | 1 | 21.29 ± 0.23 | — | 20.67 ± 0.06 | 2.97 ± 0.85 | 18.44 ± 1.24 | 15.65 ± 6.54 |
| | 2 | 96.45 ± 1.49 | — | 96.55 ± 1.62 | 0.10 ± 0.14 | 96.47 ± 1.51 | 0.02 ± 0.02 |
| | 3 | 207.79 ± 1.58 | — | 207.65 ± 1.91 | 0.08 ± 1.68 | 208.01 ± 2.11 | 0.09 ± 1.78 |
| 90° | 1 | 21.15 ± 0.02 | — | 20.45 ± 0.18 | 3.43 ± 0.79 | 19.03 ± 0.45 | 11.17 ± 2.49 |
| | 2 | 95.23 ± 3.06 | — | 95.18 ± 2.93 | 0.05 ± 0.14 | 95.11 ± 2.77 | 0.12 ± 0.30 |
| | 3 | 205.46 ± 2.62 | — | 205.42 ± 2.55 | 0.02 ± 0.03 | 205.50 ± 2.52 | 0.02 ± 0.05 |
| Isotropic | 1 | 20.91 ± 0.47 | — | 19.87 ± 0.21 | 5.25 ± 3.47 | 19.14 ± 0.33 | 9.25 ± 0.58 |
| | 2 | 96.46 ± 0.26 | — | 96.43 ± 0.36 | 0.04 ± 0.11 | 96.44 ± 0.30 | 0.02 ± 0.04 |
| | 3 | 207.91 ± 0.45 | — | 207.89 ± 0.54 | 0.01 ± 0.05 | 207.85 ± 0.35 | 0.03 ± 0.04 |

**Table 3.** Transient response and velocity of the first three-vibration modes for different magnetorheological core pre-structures and magnetic fields.

| | | Amplitude ($\mu$m s$^{-1}$) | | |
|---|---|---|---|---|
| Sample | Mode No. | 0 mT | 120 mT | 240 mT |
| 0° | 1 | 129.56 ± 0.72 | 112.18 ± 0.30 | 72.05 ± 1.47 |
| | 2 | 51.09 ± 1.69 | 49.95 ± 1.23 | 52.99 ± 1.96 |
| | 3 | 2.30 ± 0.32 | 2.79 ± 0.50 | 2.68 ± 0.29 |
| 30° | 1 | 107.73 ± 0.52 | 81.45 ± 0.31 | 51.97 ± 1.64 |
| | 2 | 63.19 ± 1.50 | 62.12 ± 1.01 | 63.48 ± 1.31 |
| | 3 | 3.06 ± 0.46 | 2.43 ± 0.24 | 2.86 ± 0.50 |
| 45° | 1 | 112.51 ± 0.34 | 87.84 ± 0.28 | 48.10 ± 0.49 |
| | 2 | 68.39 ± 1.90 | 66.38 ± 0.31 | 66.49 ± 2.20 |
| | 3 | 2.97 ± 0.49 | 2.41 ± 0.49 | 2.70 ± 0.40 |
| 90° | 1 | 125.99 ± 0.75 | 101.94 ± 0.39 | 59.15 ± 1.63 |
| | 2 | 85.48 ± 2.41 | 86.23 ± 2.93 | 86.46 ± 1.49 |
| | 3 | 3.76 ± 0.12 | 3.56 ± 0.38 | 3.23 ± 0.34 |
| Isotropic | 1 | 103.05 ± 0.63 | 91.12 ± 0.79 | 54.72 ± 2.06 |
| | 2 | 70.72 ± 2.35 | 68.46 ± 1.00 | 68.35 ± 1.99 |
| | 3 | 3.99 ± 0.45 | 4.03 ± 0.18 | 4.06 ± 0.36 |

third vibration modes did not change the resonant frequency because the metallic skin has significantly more stiffness than the magnetorheological core, and a high variation in the core stiffness would be necessary to be able to change between the second and third vibration modes [44]. Moreover, all oriented pre-structures exhibited a decrease in fundamental resonance frequency, except in other modes. The first resonance frequency mode variations of MRE-sandwich structures were compared at the highest magnetic field intensity (240 mT), and oriented pre-structures of 0°, 30°, 45°, and 90° as well as an isotropic pre-structure had variations of 16.39%, 15.17%, 15.65%, 11.17%, and 9.25%, respectively. Many studies have shown that increasing the localized magnetic field intensity decreases the first vibration mode of the MRE-sandwich beam [36, 43, 46]. Figure 9 and supplementary video 1 show the transient response of the different vibration modes for a representative sample of a 30° pre-structure of the MRE core with the variation of magnetic field intensities.

Table 3 shows the sandwich structure containing an MRE with oriented pre-structures of 0°, 30°, 45°, and 90°, and an

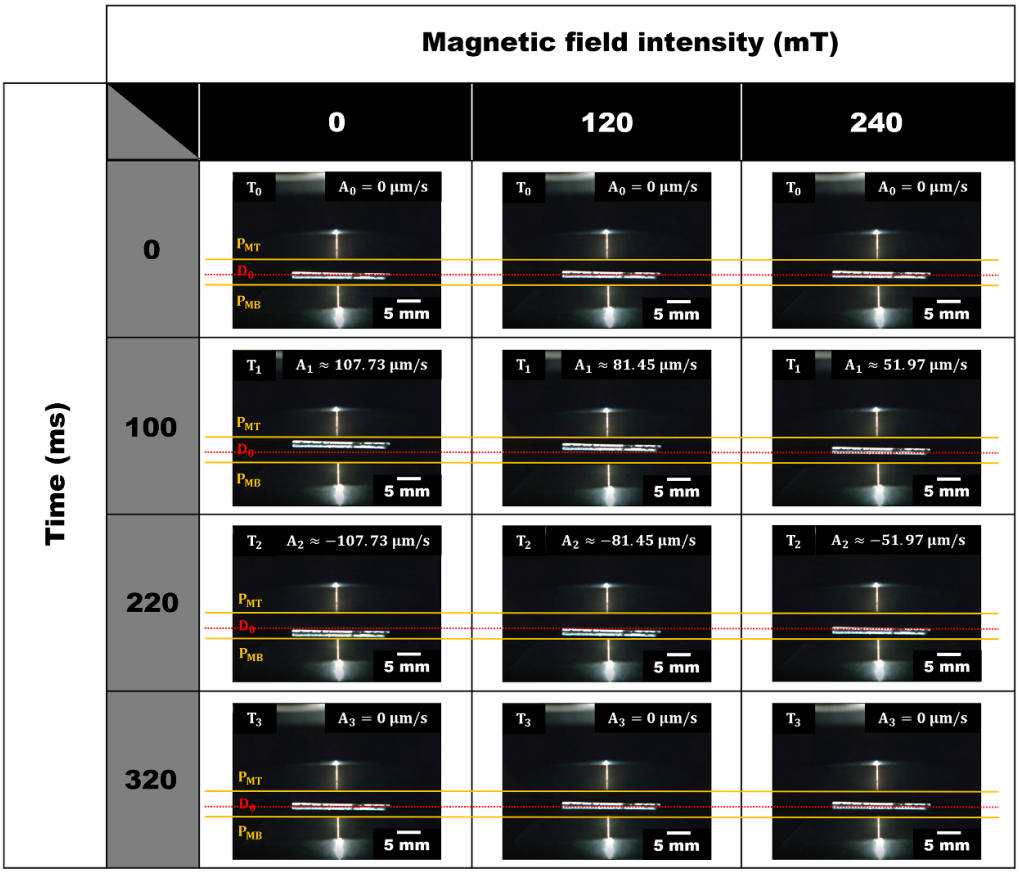


**Figure 8.** High-speed microscope images of vibrational MRE-sandwich beam under variation of magnetic field intensity for a representative sample of a 30° pre-structure of the MRE core.

isotropic pre-structure at the first three frequency modes with the variation of the magnetic field. The average amplitudes of the first vibration mode are 129.56 $\mu$m s$^{-1}$, 107.73 $\mu$m s$^{-1}$, 112.51 $\mu$m s$^{-1}$, 125.99 $\mu$m s$^{-1}$, and 103.05 $\mu$m s$^{-1}$, respectively. When the magnetic field was increased to 240 mT, the average amplitudes reduced to 72.05 $\mu$m s$^{-1}$, 51.97 $\mu$m s$^{-1}$, 48.10 $\mu$m s$^{-1}$, 59.15 $\mu$m s$^{-1}$, and 54.72 $\mu$m s$^{-1}$, respectively. The percentages of reduction in the vibration amplitude under a magnetic field of 240 mT are approximately 44%, 52%, 57%, 53%, and 47%, respectively. However, there is no interference with the second and third modes; only the first mode has been reduced. A substantial reduction in vibration amplitude is associated with an increase in the magnetic field intensity because of changing dynamic properties, as shown in figure 8 and supplementary video 2, which are correlated with figure 9(A). Therefore, the magnetic field attraction of particles according to the magnetic field intensities was responsible for the reduction in vibration magnitude.

The more significantly oriented the pre-structure of magnetic particle is, the more significant the attraction to the magnet poles as the magnetic field increases. Moreover, the larger the applied magnetic field, the greater the difficulty of any given point on the beam surface has for moving [44]. Although, the enhanced stiffening effect occurs in the MRE-core due to more extended network formation of ferromagnetic particles in the presence of a magnetic field. However, the decrease in resonance frequency can be enhanced more significantly by damping effects of MRE-core than stiffening effect. The reduction of the vibration amplitude at fundamental frequency mode is related mainly to the increase in damping capacity under a magnetic field. In addition, the increasing strain energy stored in the sandwich structure reduces the vibration amplitude.

The experiment of the MRE-damping sandwich for attenuation structural vibration for a wide frequency bandwidth is analyzed. In addition, the dynamic properties of MRE-sandwich structures depend on frequency, temperature, and strain level. All experiments in the present study were performed at environmental temperature and in the linear viscoelastic region. The experimental study was conducted to ensure the linear viscoelastic region range, which generates different input voltages. Figure 10 shows a linearity analysis of the second vibration mode of the MRE-sandwich structure under different excitation levels. The result confirms that all excitation signals maintain a linear viscoelastic region range because their stiffness and loss factors have not changed. The influence on their vibrational response and dynamics properties are represented by oriented pre-structures replacing variable magnetic field intensity to improve the damping capabilities of the MRE-sandwich structure. The effect of oriented pre-structure due to magnetic force interactions in the viscoelastic layer of the MRE sandwich is discussed.

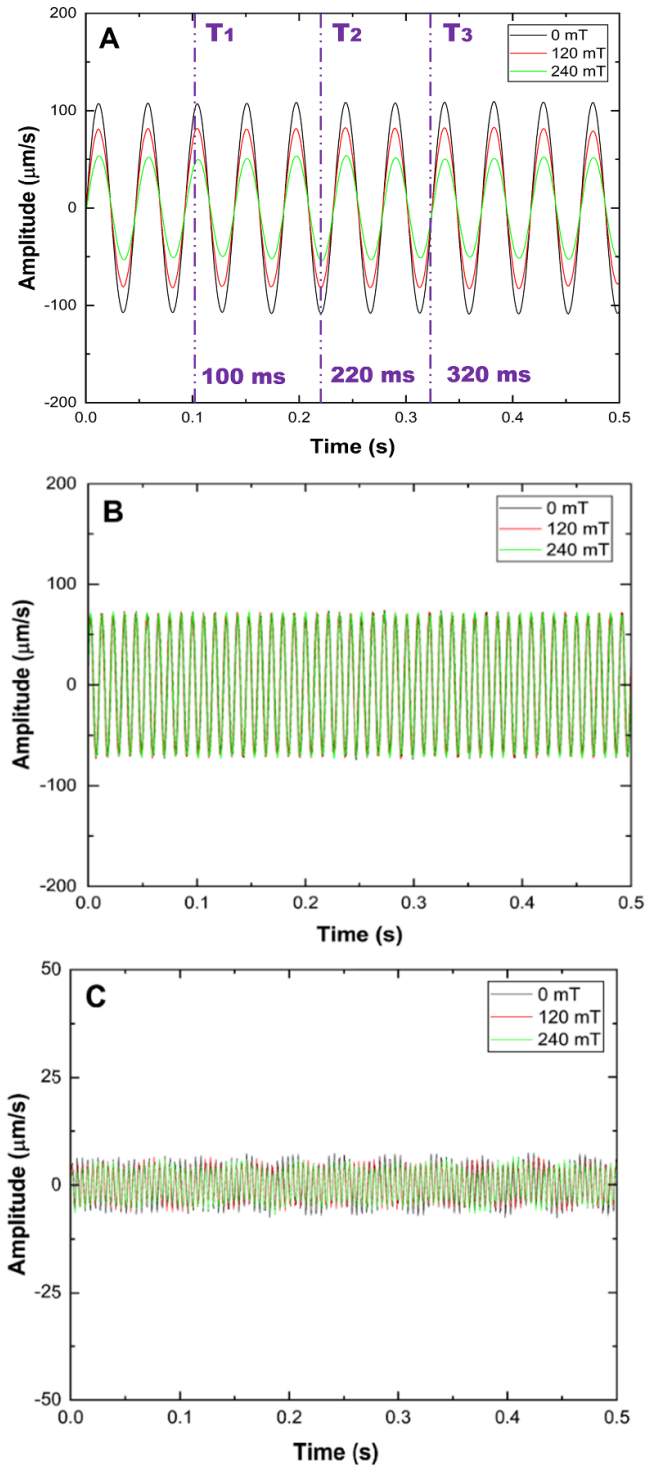


**Figure 9.** Transient response of forced vibration for the (A) first vibration mode, (B) second vibration mode, and (C) third vibration mode for a representative sample of a 30° pre-structure of the MRE core with the variation of magnetic field intensities.

The transmission function is converted by the FFT spectrum in the time response signal. Results are all averages of three specimens with their corresponding standard deviations. The transmissibility modulus within the bandwidth of 0–250 Hz of MRE-sandwich structures is shown in figure 11.

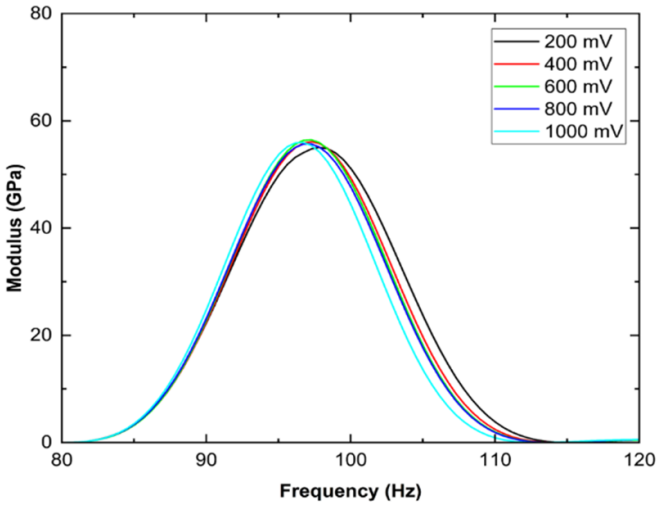


**Figure 10.** Linearity analysis of MRE-sandwich structures (second mode frequency under different excitation levels).

The induced magnetic field decreased the transmissibility modulus of the MRE-sandwich structure in the first resonance frequency significantly, whereas there was no decrement in the second or third modes. Consequently, the energy dissipation results when the MRE-sandwich structure begins vibrating by two mechanisms: shear deformation and magnetic force interaction [65]. Figure 12 shows the storage modulus and loss factor of the oriented pre-structures with variation in the magnetic field. The loss factor of MRE-sandwich structures increased gradually at the first vibration mode, whereas the storage modulus decreased significantly.

Table 4 shows the experimental dynamics properties of MRE-sandwich structures obtained from the forced vibration test with five oriented pre-structures. Experimental results show the efficiency of MRE-sandwich structures in attenuating vibration in a low frequency bandwidth with significantly modified mechanical properties. In the present study, the MRE-sandwich beam is designed with differently oriented pre-structures. The advantage of varying the orientation of pre-structure ferromagnetic particles inside the viscoelastic layer for the embedded MRE-sandwich structures is that it enhances the dynamic properties. As a result, the magneto-induced loss factors of 0°, 30°, 45°, and 90° and isotropic pre-structures increased by 30.29%, 30.93%, 32.44%, 24.46%, and 24.50%, respectively, at a magnetic field intensity of 240 mT, whereas the storage modulus was reduced by 33.66%, 32.52%, 33.24%, 23.53%, and 19.36%, respectively. Figure 13 reveals the frequency dependency of MRE-sandwich structures in which all structures have been a sharp decline in storage modulus and loss factor. In contrast, all oriented pre-structures of the MRE-layer exhibit a clear growth trend for only the shear modulus, as shown in figure 14. The loss factor of the MRE layer is higher than that of the sandwich structures by approximately 200%, especially in the first vibration mode. It is concluded that the MRE-layer has sufficient dissipated energies from structural vibration. In addition, the considerable oriented pre-structures in the MRE-layer

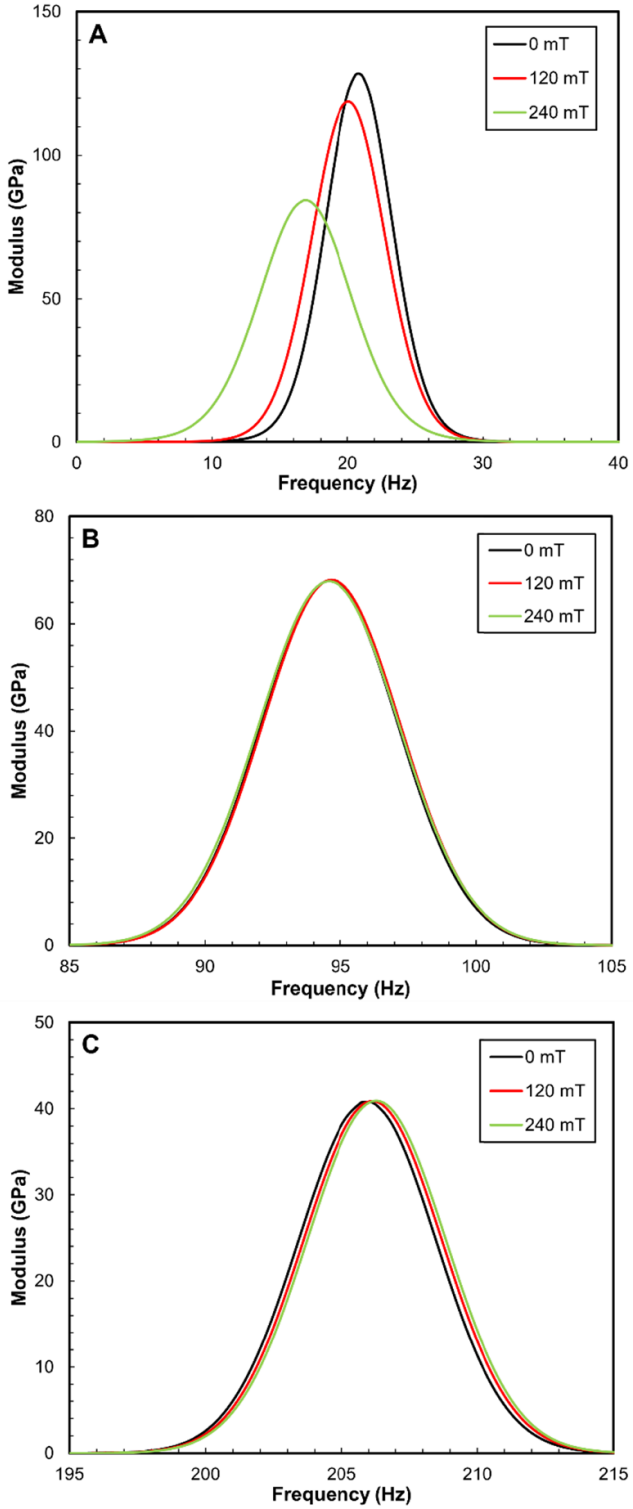


**Figure 11.** Transmission function of the MRE sandwich with magnetic field dependence. (A) First mode, (B) second mode, and (C) third mode of vibration.

presented an extraordinary capacity for changing the dynamic properties. The dynamic properties of the MRE layer obtained from the forced vibration test with five oriented pre-structures are listed in table 5.

These experimental results indicated that when the sandwich vibrates in a magnetic field, several effects occur. Firstly, as the core is MRE, it changes its dynamic properties (stiffness and loss factor in the presence of a magnetic field) as a function of the oriented pre-structure. Secondly, as metallic layers are made from aluminum, when they vibrate in the presence of a magnetic field, Eddy current appears, affecting the mechanical properties. Finally, the elastic and magnetic effects are

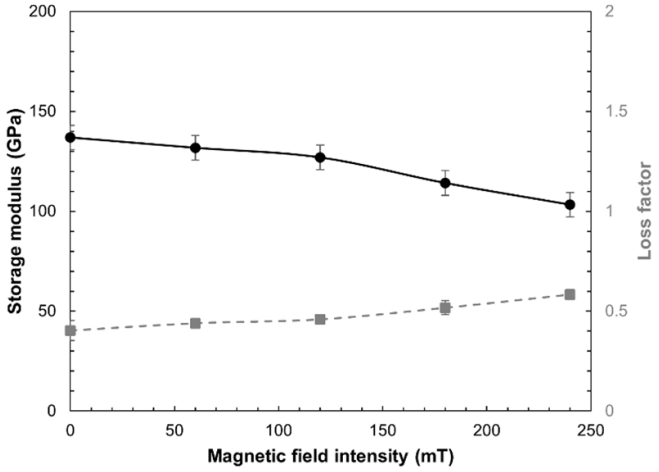


**Figure 12.** Experimental dynamic properties, (●) storage modulus and (■) loss factor, of the MRE-sandwich structure of 0° oriented pre-structure on magnetic field intensity dependence.

**Table 4.** Dynamics properties of MRE-sandwich structures.

| | | Magnetic field intensity (mT) | | | | | |
|---|---|---|---|---|---|---|---|
| | | 0 | | 120 | | 240 | |
| Sample | Mode No. | $E$ (GPa) | $\eta$ | $E$ (GPa) | $\eta$ | $E$ (GPa) | $\eta$ |
| 0° | 1 | 131.95 ± 4.86 | 0.39 ± 0.01 | 124.50 ± 7.39 | 0.44 ± 0.01 | 98.72 ± 21.03 | 0.56 ± 0.10 |
| | 2 | 67.98 ± 4.61 | 0.16 ± 0.05 | 68.05 ± 4.80 | 0.16 ± 0.05 | 67.90 ± 4.68 | 0.16 ± 0.04 |
| | 3 | 41.87 ± 1.13 | 0.10 ± 0.05 | 42.02 ± 1.23 | 0.09 ± 0.05 | 42.18 ± 1.48 | 0.09 ± 0.05 |
| 30° | 1 | 140.07 ± 4.48 | 0.40 ± 0.01 | 129.01 ± 2.94 | 0.45 ± 0.01 | 109.27 ± 8.33 | 0.58 ± 0.02 |
| | 2 | 69.26 ± 3.17 | 0.17 ± 0.01 | 69.19 ± 3.39 | 0.17 ± 0.01 | 69.31 ± 3.07 | 0.17 ± 0.01 |
| | 3 | 41.07 ± 0.56 | 0.11 ± 0.01 | 41.02 ± 0.54 | 0.11 ± 0.02 | 41.08 ± 0.51 | 0.11 ± 0.02 |
| 45° | 1 | 129.04 ± 2.83 | 0.37 ± 0.05 | 121.69 ± 0.67 | 0.42 ± 0.03 | 96.85 ± 13.07 | 0.55 ± 0.09 |
| | 2 | 67.46 ± 2.08 | 0.17 ± 0.01 | 67.70 ± 2.27 | 0.18 ± 0.01 | 67.48 ± 2.11 | 0.18 ± 0.01 |
| | 3 | 39.94 ± 0.61 | 0.10 ± 0.03 | 39.88 ± 0.73 | 0.10 ± 0.03 | 40.02 ± 0.81 | 0.10 ± 0.03 |
| 90° | 1 | 126.07 ± 0.25 | 0.41 ± 0.02 | 117.87 ±2.04 | 0.47 ± 0.01 | 102.06 ± 4.78 | 0.54 ± 0.05 |
| | 2 | 65.10 ± 4.19 | 0.15 ± 0.01 | 65.04 ± 4.00 | 0.15 ± 0.01 | 64.95 ± 3.79 | 0.15 ± 0.01 |
| | 3 | 38.66 ± 0.98 | 0.09 ± 0.03 | 38.64 ± 0.96 | 0.09 ± 0.04 | 38.67 ± 0.95 | 0.09 ± 0.04 |
| Isotropic | 1 | 118.80 ± 5.56 | 0.37 ± 0.01 | 110.79 ± 2.29 | 0.42 ± 0.03 | 102.80 ± 3.57 | 0.50 ± 0.02 |
| | 2 | 66.52 ± 0.35 | 0.18 ± 0.01 | 66.47 ± 0.50 | 0.18 ± 0.01 | 66.49 ± 0.41 | 0.18 ± 0.01 |
| | 3 | 39.41 ± 0.17 | 0.11 ± 0.01 | 39.41 ± 0.21 | 0.11 ± 0.01 | 39.39 ± 0.13 | 0.11 ± 0.01 |

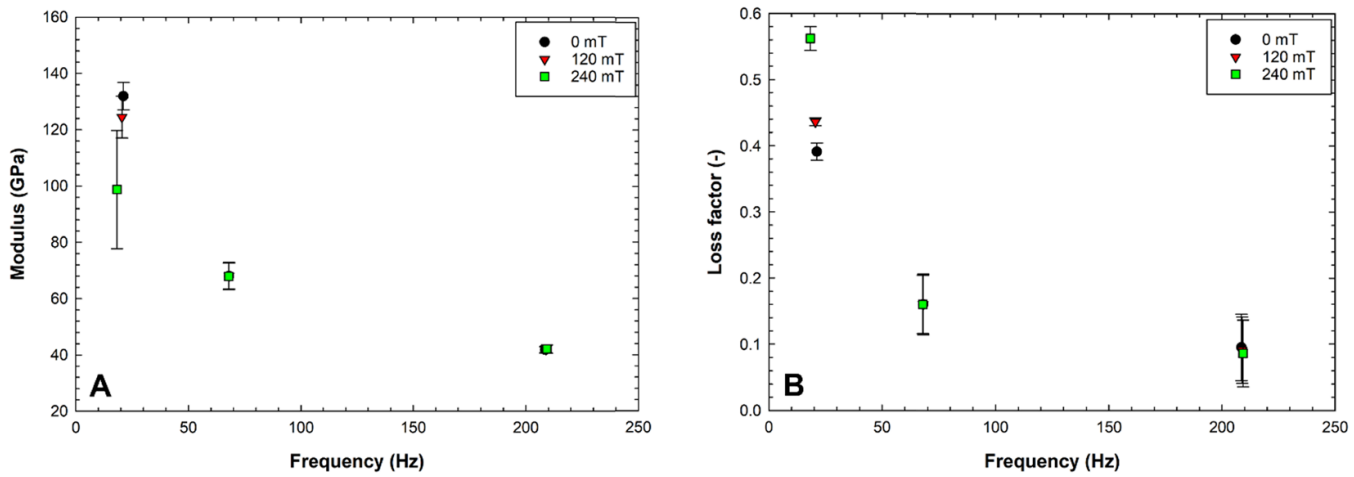


**Figure 13.** Experimental dynamic properties, 0 mT (●), 120 mT (▼), and 240 mT (■), of the MRE- sandwich structure of 0° oriented pre-structure specimen in frequency domain. (A) Storage modulus and (B) loss factor.

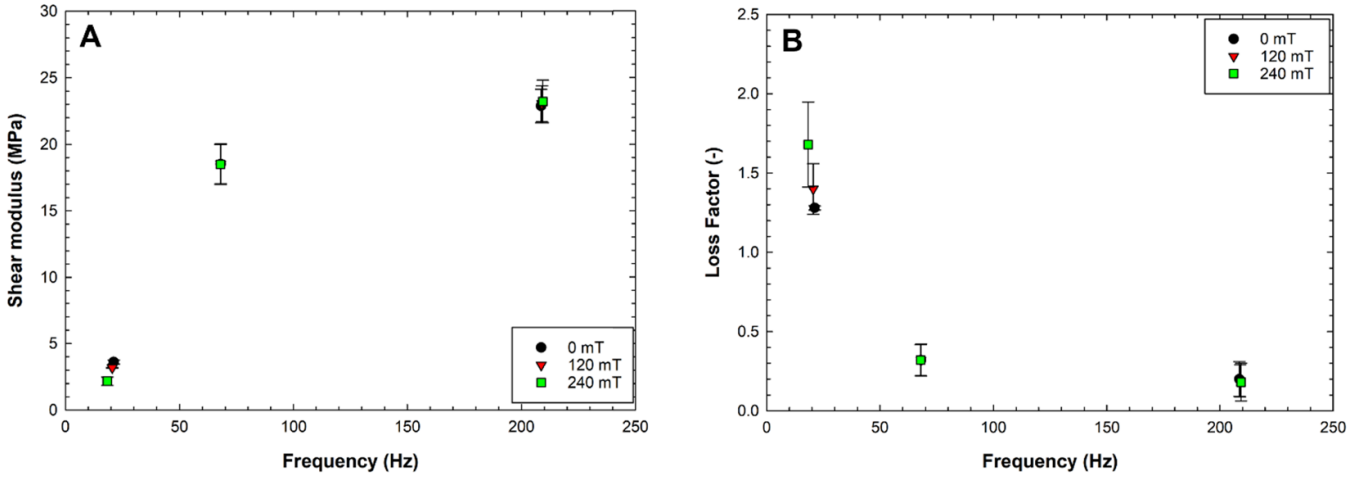


**Figure 14.** Experimental dynamic properties, 0 mT (●), 120 mT (▼), and 240 mT (■), of the MRE layer of the 0° oriented pre-structure specimen in the frequency domain. (A) Shear modulus and (B) loss factor.

**Table 5.** Dynamics properties of the MRE-layer.

| | | Magnetic field intensity (mT) | | | | | |
|---|---|---|---|---|---|---|---|
| | | 0 | | 120 | | 240 | |
| Sample | Mode No. | $G_v$ (MPa) | $\eta_v$ | $G_v$ (MPa) | $\eta_v$ | $G_v$ (MPa) | $\eta_v$ |
| 0° | 1 | 3.61 ± 0.16 | 1.28 ± 0.01 | 3.18 ± 0.03 | 1.40 ± 0.16 | 2.17 ± 0.31 | 1.68 ± 0.27 |
| | 2 | 18.51 ± 1.47 | 0.32 ± 0.10 | 18.52 ± 1.54 | 0.32 ± 0.10 | 18.49 ± 1.51 | 0.32 ± 0.10 |
| | 3 | 22.88 ± 1.27 | 0.20 ± 0.11 | 23.05 ± 1.35 | 0.19 ± 0.10 | 23.22 ± 1.61 | 0.18 ± 0.12 |
| 30° | 1 | 3.51 ± 0.07 | 1.47 ± 0.07 | 2.99 ± 0.08 | 1.61 ± 0.01 | 2.11 ± 0.16 | 1.89 ± 0.04 |
| | 2 | 18.79 ± 1.19 | 0.36 ± 0.01 | 18.77 ± 1.28 | 0.35 ± 0.01 | 18.82 ± 1.15 | 0.35 ± 0.01 |
| | 3 | 21.48 ± 0.60 | 0.24 ± 0.03 | 21.43 ± 0.59 | 0.24 ± 0.04 | 21.49 ± 0.56 | 0.24 ± 0.04 |
| 45° | 1 | 3.80 ± 0.30 | 1.17 ± 0.26 | 3.36 ± 0.21 | 1.27 ± 0.16 | 2.35 ± 0.57 | 1.54 ± 0.26 |
| | 2 | 18.92 ± 0.83 | 0.35 ± 0.01 | 18.97 ± 0.91 | 0.35 ± 0.01 | 18.91 ± 0.84 | 0.35 ± 0.01 |
| | 3 | 22.15 ± 0.53 | 0.21 ± 0.07 | 22.09 ± 0.83 | 0.22 ± 0.07 | 22.23 ± 0.92 | 0.22 ± 0.08 |
| 90° | 1 | 3.51 ± 0.17 | 1.30 ± 0.12 | 2.99 ± 0.03 | 1.48 ± 0.08 | 2.45 ± 0.28 | 1.57 ± 0.16 |
| | 2 | 18.46 ± 1.66 | 0.29 ± 0.01 | 18.40 ± 1.54 | 0.30 ± 0.02 | 18.36 ± 1.46 | 0.30 ± 0.02 |
| | 3 | 21.45 ± 0.94 | 0.18 ± 0.07 | 21.43 ± 0.91 | 0.18 ± 0.07 | 21.46 ± 0.90 | 0.19 ± 0.07 |
| Isotropic | 1 | 3.66 ± 0.08 | 1.10 ± 0.09 | 3.13 ± 0.11 | 1.16 ± 0.15 | 2.62 ± 0.15 | 1.38 ± 0.04 |
| | 2 | 18.46 ± 0.06 | 0.36 ± 0.02 | 18.44 ± 0.10 | 0.36 ± 0.03 | 18.44 ± 0.06 | 0.36 ± 0.03 |
| | 3 | 21.19 ± 0.19 | 0.23 ± 0.01 | 21.18 ± 0.23 | 0.23 ± 0.02 | 21.16 ± 0.15 | 0.23 ± 0.01 |

coupled when the component is vibrating in the presence of a magnetic because the core is magnetic, whereas the layer is not [65].

## 4. Conclusions

In this study, we presented five oriented pre-structures of the MRE-sandwich structure, experimentally investigated the viscoelastic properties of MRE, and analyzed the dynamic properties of MRE-sandwich structures according to the ASTM E756-05 standard [61] with the modification proposed by Cortés and Elejabarrieta [63].

Viscoelastic properties of each oriented pre-structure MRE were observed. Rheological properties depended entirely on the pre-structure because the alignment of the internal structure induced storage modulus and loss factor. The magnetic field was found more effective in increasing the stiffness of MREs.

The vibration response and dynamic properties of MRE-sandwich structures were analyzed for the entire frequency bandwidth between 0 and 250 Hz. Oriented pre-structures of the MRE layer attenuated vibration slightly across the low frequency bandwidth such that the layer dissipated energy via the microstructure of the viscoelastic layer by shearing deformation. The magnetic field intensity shows significant vibration

suppression at low frequencies because of the magneto-elastic effect and magnetic effect [65].

Results also highlight that the proposed MRE-sandwich structures can be used to avoid unwanted resonances, especially at the first vibration mode, thereby reducing failures due to excessive vibration and enhancing the damping properties due to dissipated energy.

In conclusion, the proposed oriented pre-structure of the MRE-sandwich demonstrated good vibration attenuation performance due the change in their stiffness by application of a magnetic field. In addition, optical micrographs clearly showed the structural motion of vibration attenuation of the MRE sandwich under magnetic field intensities. The vibration attenuation in the MRE sandwich with variation of the core pre-structures is of utmost importance in order to use such MRE sandwiches as acoustic vibration devices in vibration control systems.

## Data availability statement

All data that support the findings of this study are included within the article (and any supplementary files).

## Acknowledgments

The authors gratefully acknowledge Mr Keita Saito, Department of Mechanical Engineering, Nagaoka University of Technology for conducting the magnetorheological measurements.

## Conflict of interest

The authors declare that there is no conflict of interest with respect to the research and/or publication of this paper.

## Funding

This research did not receive any specific grant from funding agencies in the public, commercial, or not-for-profit sectors.

## ORCID iDs

Narongdet Sulatchaneenopdon https://orcid.org/0000-0002-2239-7518
Zhiming Shen https://orcid.org/0000-0003-1246-7954
Hyoung-Won Son https://orcid.org/0000-0002-2047-644X
Anak Khantachawana https://orcid.org/0000-0002-8460-6645
Jon Garcia-Barruetabena https://orcid.org/0000-0002-2483-7038
Maria Jesus Elejabarrieta https://orcid.org/0000-0001-8908-2193
Tadachika Nakayama https://orcid.org/0000-0001-6880-8936

## References

[1] Rao M D 2003 Recent applications of viscoelastic damping for noise control in automobiles and commercial airplanes *J. Sound Vib.* **262** 457–74
[2] Garg D P, Zikry M A and Anderson G L 2001 Current and potential future research activities in adaptive structures: an ARO perspective *Smart Mater. Struct.* **10** 610–23
[3] Chen L, Gong X L, Jiang W Q, Yao J J, Deng H X and Li W H 2007 Investigation on magnetorheological elastomers based on natural rubber *J. Mater. Sci.* **42** 5483–9
[4] Feng J, Xuan S, Liu T, Ge L, Yan L, Zhou H and Gong X 2015 The prestress-dependent mechanical response of magnetorheological elastomers *Smart Mater. Struct.* **24** 085032
[5] Ginder J M, Clark S M, Schlotter W F and Nichols M E 2001 Magnetostrictive phenomena in magnetorheological elastomers *Int. J. Mod. Phys.* B **16** 2412–8
[6] Hu Y, Wang Y L, Gong X L, Gong X Q, Zhang X Z, Jiang W Q and Chen Z Y 2005 New magnetorheological elastomers based on polyurethane/Si-rubber hybrid *Polym. Test.* **24** 324–9
[7] Lee C W, Kim I H and Jung H J 2018 Fabrication and characterization of natural rubber-based magnetorheological elastomers at large strain for base isolators *Shock Vib.* **2018** 7434536
[8] Leng J 2014 Magnetorheology: advances and applications, edited by Norman M Wereley *Int. J. Smart Nano Mater.* **5** 33
[9] Li Y and Li J 2015 Finite element design and analysis of adaptive base isolator utilizing laminated multiple magnetorheological elastomer layers *J. Intell. Mater. Syst. Struct.* **26** 1861–70
[10] Liu T, Gong X, Xu Y, Xuan S and Jiang W 2013 Simulation of magneto-induced rearrangeable microstructures of magnetorheological plastomers *Soft Matter* **9** 10069–80
[11] Jolly M R, Carlson J D and Muñoz B C 1996 A model of the behaviour of magnetorheological materials *Smart Mater. Struct.* **5** 607–14
[12] Lokander M and Stenberg B 2003 Performance of isotropic magnetorheological rubber materials *Polym. Test.* **22** 245–51
[13] Rosenzweig R 1985 *Ferrohydrodynamics* (Cambridge: Cambridge University Press)
[14] Schubert G and Harrison P 2016 Magnetic induction measurements and identification of the permeability of magnetorheological elastomers using finite element simulations *J. Magn. Magn. Mater.* **404** 205–14
[15] Kumar V, Lee J Y and Lee D J 2018 The response force and rate of magnetorheological elastomers with different fillers and magnetic fields *J. Magn. Magn. Mater.* **466** 164–71
[16] Bastola A K, Paudel M and Li L 2018 Magnetic circuit analysis to obtain the magnetic permeability of magnetorheological elastomers *J. Intell. Mater. Syst. Struct.* **29** 2946–53
[17] Boczkowska A, Awietjan S F, Pietrzko S and Kurzydłowski K J 2012 Mechanical properties of magnetorheological elastomers under shear deformation *Composites* B **43** 636–40
[18] Agirre-Olabide I, Kuzhir P and Elejabarrieta M J 2018 Linear magneto-viscoelastic model based on magnetic permeability components for anisotropic magnetorheological elastomers *J. Magn. Magn. Mater.* **446** 155–61
[19] Tian T and Nakano M 2018 Fabrication and characterisation of anisotropic magnetorheological elastomer with 45° iron particle alignment at various silicone oil concentrations *J. Intell. Mater. Syst. Struct.* **29** 151–9
[20] Zhang J, Pang H, Wang Y and Gong X 2020 The magneto-mechanical properties of off-axis anisotropic

magnetorheological elastomers *Compos. Sci. Technol.* **191** 108079
[21] Kerwin E 1959 M1959 damping of flexural waves by a constrained viscoelastic layer *J. Acoust. Soc.* **31** 952–62
[22] Ungar E E 1962 Loss factors of viscoelastically damped beam structures *J. Acoust. Soc.* **34** 1082–9
[23] Zheng C, Yan S and Liu B 2022 Investigation on dynamic characteristics of composite sandwich plates with co-cured damping core *Appl. Acoust.* **192** 108735
[24] Irazu L and Elejabarrieta M J 2017 The effect of the viscoelastic film and metallic skin on the dynamic properties of thin sandwich structures *Compos. Struct.* **176** 407–19
[25] Martinez-Agirre M and Elejabarrieta M J 2010 Characterisation and modelling of viscoelastically damped sandwich structures *Int. J. Mech. Sci.* **52** 1225–33
[26] Leibowitz M and Lifshitz J M 1990 Experimental verification of modal parameters for 3-layered sandwich beams *Int. J. Solids Struct.* **26** 175–84
[27] Teng T L and Hu N K 2001 Analysis of damping characteristics for viscoelastic laminated beams *Comput. Methods Appl. Mech. Eng.* **190** 3881–92
[28] Daya E M, Azrar L and Potier-Ferry M 2004 An amplitude equation for the non-linear vibration of viscoelastically damped sandwich beams *J. Sound Vib.* **271** 789–13
[29] Alijani F and Amabili M 2014 Non-linear static bending and forced vibrations of rectangular plates retaining non-linearities in rotations and thickness deformation *Int. J. Non-Linear Mech.* **67** 394–04
[30] Amabili M 2016 Nonlinear vibrations of viscoelastic rectangular plates *J. Sound Vib.* **362** 142–56
[31] Araújo A L, Mota Soares C M, Mota Soares C A and Herskovits J 2010 Optimal design and parameter estimation of frequency dependent viscoelastic laminated sandwich composite plates *Compos. Struct.* **92** 2321–7
[32] Hamdaoui M, Robin G, Jrad M and Daya E M 2015 Optimal design of frequency dependent three-layered rectangular composite beams for low mass and high damping *Compos. Struct.* **120** 174–82
[33] Madeira J F A, Araújo A L, Mota Soares C M, Mota Soares C A and Ferreira A J M 2015 Multiobjective design of viscoelastic laminated composite sandwich panels *Composites* B **77** 391–01
[34] Madeira J F A, Araújo A L, Mota Soares C M and Mota Soares C A 2015 Multiobjective optimization of viscoelastic laminated sandwich structures using the direct MultiSearch method *Comput. Struct.* **147** 229–35
[35] Kolekar S, Venkatesh K, Oh J and Choi S 2019 Vibration controllability of sandwich structures with smart materials of electrorheological fluids and magnetorheological materials: a review *J. Vib. Eng. Technol.* **7** 359–377
[36] Lara-Prieto V, Parkin R, Jackson M, Silberschmidt V and Kęsy Z 2010 Vibration characteristics of MR cantilever sandwich beams: experimental study *Smart Mater. Struct.* **19** 015005
[37] Irazu L and Elejabarrieta M J 2017 Magneto-dynamic analysis of sandwiches composed of a thin viscoelastic-magnetorheological layer *J. Intell. Mater. Syst. Struct.* **28** 3106–14
[38] Wei K, Bai Q, Meng G and Ye L 2011 Vibration characteristics of electrorheological elastomer sandwich beams *Smart Mater. Struct.* **20** 055012
[39] Ramkumar K and Ganesan N 2009 Vibration and damping of composite sandwich box column with viscoelastic/electrorheological fluid core and performance comparison *Mater. Des.* **30** 2981–94
[40] Eshaghi M, Sedaghati R and Rakheja S 2016 Dynamic characteristics and control of magnetorheological/electrorheological sandwich structures: a state-of-the-art review *J. Intell. Mater. Syst. Struct.* **27** 2003–37
[41] Butaud P, Foltête E and Ouisse M 2016 Sandwich structures with tunable damping properties: on the use of shape memory polymer as viscoelastic core *Compos. Struct.* **153** 401–8
[42] Yeh J Y 2013 Vibration analysis of sandwich rectangular plates with magnetorheological elastomer damping treatment *Smart Mater. Struct.* **22** 035010
[43] Hu G, Guo M, Li W, Du H and Alici G 2011 Experimental investigation of the vibration characteristics of a magnetorheological elastomer sandwich beam under non-homogeneous small magnetic fields *Smart Mater. Struct.* **20** 127001
[44] de Souza Eloy F, Gomes G F, Ancelotti A C, da Cunha S S, Bombard A J F and Junqueira D M 2018 Experimental dynamic analysis of composite sandwich beams with magnetorheological honeycomb core *Eng. Struct.* **176** 231–42
[45] Choi W J, Xiong Y P and Shenoi R A 2010 Vibration characteristics of sandwich beams with steel skins and magnetorheological elastomer cores *Adv. Struct. Eng.* **13** 837–47
[46] Hu G L, Guo M and Li W H 2011 Analysis of vibration characteristics of magnetorheological elastomer sandwich beam under non-homogeneous magnetic field *Appl. Mech. Mater.* **101–102** 202–6
[47] Chikh N, Nour A, Aguib S and Tawfiq I 2016 Dynamic analysis of the non-linear behavior of a composite sandwich beam with a magnetorheological elastomer core *Acta Mech. Solida Sin.* **29** 271–83
[48] Aguib S, Nour A, Zahloul H, Bossis G, Chevalier Y and Lançon P 2014 Dynamic behavior analysis of a magnetorheological elastomer sandwich plate *Int. J. Mech. Sci.* **87** 118–36
[49] Gurgen S and Sofuoglu M 2020 Vibration attenuation of sandwich structures filled with shear thickening fluids *Composites* B **186** 107831
[50] Rokn-Abadi M, Shahali P and Haddadpour H 2020 Effecs of magnetoelstic loads on free vibration characteristics of magnetorheological-based sandwich beam *J. Intell. Mater. Syst. Struct.* **31** 1015–28
[51] Li H, Wang W, Wang X, Han Q, Liu J, Qin Z, Xiong J and Guan Z 2020 A nonlinear analytical model of composite plate structure with an MRE function layer considering internal magnetic and temperature fields *Compos. Sci. Technol.* **200** 108445
[52] Zhang J, Yildirim T, Neupane G P, Tao Y, Bingnong J and Li W 2020 Experimental dynamic performance of an aluminium-MRE shallow shell *Smart Struct. Syst.* **25** 57–64
[53] Subramani M, Ramamoorthy M, Arumugam A B and Selvaraj R 2021 Free and forced vibration characteristics of CNT reinforced composite spherical sandwich shell panels with MR elastomer core *Int. J. Struct. Stab. Dyn.* **21** 2150136
[54] Selvaraj R, Ramamoorthy M and Arumugam A B 2021 Experimental and numerical studies on dynamic performance of the rotating composite sandwich panel with CNT reinforced MR elastomer core *Compos. Struct.* **277** 114560
[55] Wang Y, Yang J, Chen Z, Gong X, Du H, Zhang S, Li W and Sun S 2022 Investigation of a novel MRE metamaterial sandwich beam with real-time tunable band gap characteristics *J. Sound Vib.* **527** 116870
[56] Arani A G, Shahraki M E and Haghparast E 2022 Instability analysis of axially moving sandwich plates with a magnetorheological elastomer core and GNP-

reinforced face sheets *J. Braz. Soc. Mech. Sci.* **44** 1556–79
[57] Li H, Wang W, Wang Q, Han Q, Liu J, Qin Z, Xiong J and Wang X 2022 Static and dynamic performances of sandwich plates with magnetorheological elastomer core: theoretical and experimental studies *J. Sandw. Struct. Mater.* **24** 1556–79
[58] Sharif U, Sun B, Hussain S, Ibrahim D S, Adewale O O, Ashraf S and Bashir F 2021 Dynamic behavior of sandwich structures with magnetorheological elastomer: a review *Materials* **14** 7025
[59] Irazu L and Elejabarrieta M J 2018 A novel hybrid sandwich structure: viscoelastic and eddy current damping *Mater. Des.* **140** 460–72
[60] Vemuluri R B, Rajamohan V and Arumugam A B 2018 Dynamic characterization of tapered laminated composite sandwich plates partially treated with magnetorheological elastomer *J. Sandw. Struct. Mater.* **20** 308–50
[61] ASTM 2017 ASTM E756-05: standard test method for measuring vibration damping properties of material
[62] Sulatchaneenopdon N, Son H, Khantachawana A, Garcia-Barruetabena J, Elejabarrieta M Jesus, Takahashi T, Nakayama T and Niihara K 2022 Influence of pre-structure orientation on the linear viscoelastic limit of magnetorheological elastomers *J. Intell. Mater. Syst. Struct.* 1045389X2210943
[63] Cortés F and Elejabarrieta M J 2007 Viscoelastic materials characterisation using the seismic response *Mater. Des.* **28** 2054–62
[64] Agirre-Olabide I, Berasategui J, Elejabarrieta M J and Bou-Ali M M 2014 Characterization of the linear viscoelastic region of magnetorheological elastomers *J. Intell. Mater. Syst. Struct.* **25** 2074–81
[65] Irazu L and Elejabarrieta M J 2019 Effect of magneto-elastic force on magneto-dynamic model of viscoelastic-magnetorheological sandwiches *Smart Mater. Struct.* **28** 075022